

Influence of Take-up Speeds on the Structure, Properties and Dyeability of Novel Polyamide 5,6 As-spun Fibers

Yassir A. Eltahir^{1,2}, Rabie A. M. Asad², Yumin Xia¹, Yanping Wang¹, and Wang Yimin¹

¹College of Materials Science and Engineering, State Key Laboratory for Modification of Chemical Fibers and Polymer Materials, Donghua University, 2999 North Renmin Road, Songjiang, Shanghai 201620, P.R. China.

²Faculty of Industries Engineering and Technology, University of Gezira, Wad-Medani, P.O. Box 20, Sudan.

ABSTRACT

Polyamide 5,6 (PA56) as-spun fibers were successfully prepared by melt spinning process and the effects of different take-up speeds on their thermal properties, crystalline structure and dyeability were investigated by differential scanning calorimetry (DSC), wide-angle X-ray diffraction (WAXD), dynamic mechanical thermal analysis (DMTA), sonic velocity and color strength measurements. DSC results revealed that the glass transition temperature (T_g) of PA56 as-spun fibers increased, while the melting temperature showed no considerable variation with the take-up speed. DMTA results demonstrated that the storage modulus increased, while the peak height of $\tan \delta$ decreased with take-up speeds. The equatorial (WAXD) pattern of PA56 shows α -like structure, as observed for other odd-even nylons such as nylon 5,10, nylon 9,2 and so on. It is also found that the relative crystallinity, apparent crystal sizes and molecular orientation of PA56 as-spun fibers increased with take-up speeds. As a result, the dyebath exhaustion and color strength (K/S) values decreased with the take-up speeds.

Keywords: Polyamide 5,6; As-spun fibers; Take-up speeds; Crystallinity; Color strength (K/S).

INTRODUCTION

Since the invention of nylon 66 by Carothers in 1934 (Carothers, 1938; Carothers and Graves, 1939), many kinds of nylons have been investigated and a number of them have been commercialized. Polyamides (PAs), commonly referred as nylons, are semi-crystalline polymers that can be used as fibers and engineering materials because of their unique properties, such as high modulus, high strength and toughness, and excellent resistance to abrasion (Anton & Baird, 2002; Kohan, 1995). However, it is known that many of the commonly used polyamides like polyamide 6 (Rahbar & Haji, 2013) and polyamide 66 (Danford *et al.*, 1978) are based on petrochemical building blocks. Due to the resource problems and pollution, bio-based-derived chemicals offers an enormous potential to replace the depleting fossil feedstock and are considered as an environmental friendly alternative. The use of the 1,5-pentanediamine obtained from microbial biosynthesis transformation from lysine provides partially or entirely bio-based polyamides (Kind *et al.*, 2014; Kind & Wittmann, 2011). Therefore, polyamide 5,6 fibers with high moisture absorption and release cool feeling, good wear resistance, good mechanical properties can be used as a promising alternative to conventional polyamide 6, and polyamide 66, for the textile industry. Therefore, the preparation of polyamide 5,6 fibers have some innovation and significance.

The process of melt spinning and subsequent drawing of synthetic fibers dates from pioneering efforts of Carothers and his colleagues in 1932 (Carothers & Hill, 1932; Carothers *et al.*, 1933). It has been an important manufacturing process since commercialization of nylon 66 fibers in 1940 (Bolton, 1942). Most relevant features of the influence of melt spinning and drawing variables were noted by Carothers and Hill (Carothers & Hill, 1932) such as the effect of take-up velocity on crystalline orientation and mechanical properties. Since that work, many studies have been carried out to investigate the structural changes of nylon fibers produced at various spinning speeds (Bankar *et al.*, 1977; Danford *et al.*, 1978; Samon *et al.*, 1999; Stepaniak *et al.*, 1979). Bankar *et al.* (Bankar *et al.*, 1977) investigated the relationship of the crystalline orientation of spun fibers with their spinning speed in the range of 100 - 1000 m/min. Stepaniak *et al.* (Stepaniak *et al.*, 1979) described a methods for calculating crystallinity indices and crystalline orientation functions for nylon 6 fibers at spinning speeds of 20-2435 m/min. Samon *et al.* (Samon *et al.*, 1999) studied the structure development during melt spinning of nylon 6 fibers as a function of take-up speed by on-line WAXD. They have reported that the crystalline index and crystalline orientation increases as the take-up speed increases.

Most polyamide fibers are currently dyed either with acid dyes or disperses dyes. The dyeing behavior of polyamide fibers mainly depends on their microstructures. Dyeing process is a thermally activated process and sensitive to segmental mobility of the amorphous regions, amorphous volume per crystallites, crystallinity regions, chain folding, and orientation of the amorphous phase (Atavet *et al.*, 2006; Vasanthan and Huang, 2003).

The crystal structure of nylons have been classified, according to Kinoshita (Kinoshita, 1959b), into two main forms, the α and γ forms. The α -structure, which is characterized by a fully extended planar zigzag conformation of the molecular chains, is typically observed for both even-even nylons (nylon 66) and even nylons (nylon 6) with a low number of methylene groups

(Bunn and Garner, 1947). Diffraction patterns of α -structure are mainly characterized by two strong reflections at approximately 0.44 and 0.37 nm, which are related to the spacing between crystallographic planes constituted of non-hydrogen bonded and hydrogen bonded molecules, respectively. On other hand, the γ -form, which was firstly suggested by Kinoshita (Kinoshita, 1959a), is common for nylon with more than seven carbon atoms and even-odd, odd-even and odd-odd nylons. The γ -structure exhibits a chain close to hexagonal packing with a fiber diffraction patterns characterized by a single strong equatorial reflection at approximately 0.415 nm. Transformations between both kinds of structures can be engineered in some cases by solvent or swelling agents (Arimoto, 1964), rates of spinning (Ziabicki and Kedzierska, 1959), and temperature (Luet *et al.*, 2013). However, up to now, only a few studies have been reported on the polyamide 5,6 (PA56). Puiggalí *et al.* (Puiggalí *et al.*, 1998) studied the crystal structures of PA56 and reported the lattice of the mono-clinic unit cell with: $a = 0.512$ nm, $b = 0.868$ nm, c (chain axis) = 3.133 nm and $\beta = 125.7^\circ$. Morales-Gómez *et al.* (Morales-Gómez *et al.*, 2010) investigated the Brill transition and melt crystallization of PA56. However, the preparation, development of the structure and properties during spinning of PA56 as-spun fibers have not been investigated in depth and reported so far. The purpose of the present study is to obtain information on the structure and morphologies of PA56 fibers as well as to get insight of the dyeing behavior of PA56 fibers with acid dyes. The PA56 as-spun fibers were prepared by melt spinning process at different take-up speeds and the effects of this variation on their thermal properties, crystalline structures, molecular orientation and dyeability were investigated by DSC, WAXD, DMTA, sonic velocity and color strength measurements.

MATERIAL AND METHODS

Material

PA56 with an intrinsic viscosity of 0.68 dL/g (measured in dichloroacetic acid at 25°C), was kindly supplied by Guangdong Xinhui Meida Nylon Co. Ltd, China.

Melt spinning

Melt spinning of PA56 was carried out using a lab melt-spinning machine (Polymer ABE Engineering MATE-V, Co. Tokyo, Japan) at spinning temperature of 285 °C and different take-up speeds of 800, 1000 and 3200 m/min, respectively. The pellets were extruded through a spinneret with 36 holes each with a diameter of $D = 0.3$ mm and the length/diameter ratio L/D of 3. Prior to processing the PA56 pellets were dried in a vacuum oven firstly at 50 °C for 60 min, then 75 °C for 60 min, and finally at 110 °C for 8 h before cooling to room temperature.

Linear density

Yarn linear density (expressed in dtex, which is the mass in grams per 10,000 meters) was determined as the mass in grams of 100 m long yarns by using a measuring reel model YG085 made in China, in accordance with ASTM D 1577-96. For each sample, five readings were taken and the average is reported.

Morphological structure of PA56 as-spun fibers

The surface of the PA56 as-spun fibers were observed using a scanning electron microscope (SEM, HITACHI S-3000N) at accelerating voltage of 10 kV.

Thermal properties

The melting point and heat of fusion of all the fibers were determined by a Perkin-Elmer Q20 (TA Instruments) differential scanning calorimeter (DSC). All samples of about 5 mg were placed in the standard aluminum pans, and the scans were carried out at a heating rate of 10°C/min under flowing nitrogen of 50 ml/min. The instrument was calibrated using pure indium.

Dynamic mechanical thermal analysis (DMTA)

Thermal mechanical measurements were performed using Q800 DMTA (TA Instruments) for the PA56 fibers. Fibers were placed in a film/fiber tension clamp with initial clamp separation of 10 mm, pretension of 10 mN, and oscillated at the frequency of 1 Hz. In all cases, the heating rate was 3 °C/min. The amplitude was selected to 100 μm in order to remain within the linear visco-elastic range. The glass transition temperature (T_g) was measured from the lower temperature limits of storage modulus and peak height of $\tan \delta$.

Wide-angle X-ray diffraction measurements (WAXD)

Wide-angle X-ray diffractions (WAXD) were performed in a Bruker AXS (D2 Phaser, Lynx Eye™, Germany). Samples were scanned using an incident x-ray with a Ni-filtered $\text{CuK}\alpha$ radiation with a wavelength of 0.154 nm in 2θ ranges from 10° to 60° at a step interval of 0.02°/s. The generator was operated at 30 KV and 10 mA.

Crystal size measurements

The crystalline size of the (020) plane was obtained from the half width of the 2θ peak at 20.6° by using the Scherrer equation (Alexander, 1969; Patterson, 1939), as shown in Eq. (1). The peaks were separated using a peak separation program before calculation.

$$D = \frac{K\lambda}{\beta \cos \theta} \quad (1)$$

Where, D is crystal size; K is a constant and is considered to be (0.89); λ is the wavelength of the X-ray (0.1542 nm); β is the width of the peak at half maximum intensity (radian); and θ is the Bragg angle.

Crystallinity measurements

The total intensity of diffraction is the summation of intensities both in crystalline regions and in amorphous regions; thus, the crystallinity of fiber is calculated as shown in Eq. (2):

$$X_c = \frac{I_c}{I_c + I_a} \times 100\% \quad (2)$$

Where X_c is the crystallinity of fiber; I_c is the sum of diffraction intensities due to the crystalline fraction and I_a is the diffraction intensities due to the amorphous fraction. It is noteworthy that the crystallinities determined by WAXD should be used as relative values other than absolute values to analyze the effect of the processing parameters.

Fiber orientation measurements

The orientation factors (f_0) of the as-spun fibers were measured using a model SCY-III sonic velocity apparatus, which was manufactured by DonghuaKaili Chemicals and Fiber Technology

Corporation, Shanghai, China. Before testing, specimen fibers with an approximately length of 100 cm were wound and clamped on a testing device with a span of 40 cm. The (f_0) values of the as-spun fibers were measured at 25 °C. A minimum of five samples of each specimen were tested, and the results of the orientation measurement were averaged.

Dyeing method

The dye used was an acid dye [C.I Acid Red 88], as shown in *Figure 1*, which was supplied by the Sinopharm Chemical Reagent Co., Ltd, China. PA56 fibers were knitted on a sock knitting machine, Z503 from 7th Textile Factory, China. The dyeing process was carried out according to previous work by Eltahir et al. (Eltahiret *al.*, 2016).

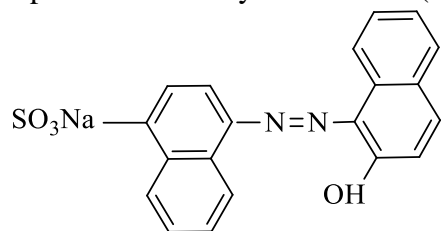


FIGURE 1. Structural Formula of C.I. Acid Red 88

Exhaustion measurement

The dye concentration of the dyebath, was measured at the wavelength of maximum absorption (at λ_{max}) before and after dyeing using a UV-Vis Spectrometer (U-3310), employing 1 cm pathlength and water as reference solvent. The dye bath exhaustions of dyes on fabrics (uptake) were calculated using Eq. (3).

$$E(\%) = \frac{(A_1 - A_2)}{A_1} \times 100 \quad (3)$$

Where E is exhaustion (%), A_1 and A_2 are absorbance (at λ_{max}) of the solutions before and after dyeing, respectively.

Measurements of color strength

The reflectance values of the dyed fabric were measured using a Datacolor spectraflash spectrophotometer (Datacolor 650, Switzerland) under illuminant D_{65} using 10° standard observers. Color strength (K/S) was calculated from the reflectance value using the well-known Kubelka-Munk Eq. (4). Each fabric was folded twice to give four thicknesses and an average of three readings was taken each time.

$$K / S = \frac{(1 - R^2)}{2R} \quad (4)$$

Where K is the coefficient of absorption, S the coefficient of scattering, and R the reflectance of the sample at given wavelength.

RESULTS AND DISCUSSION

Linear density

The effect of take-up speed on linear density of PA56 as-spun fibers is shown in *Figure 2*. Fiber linear density decreases with the increase of take-up speeds. This should be attributed to the increase of a draw down ratio with the increase of take-up speeds.

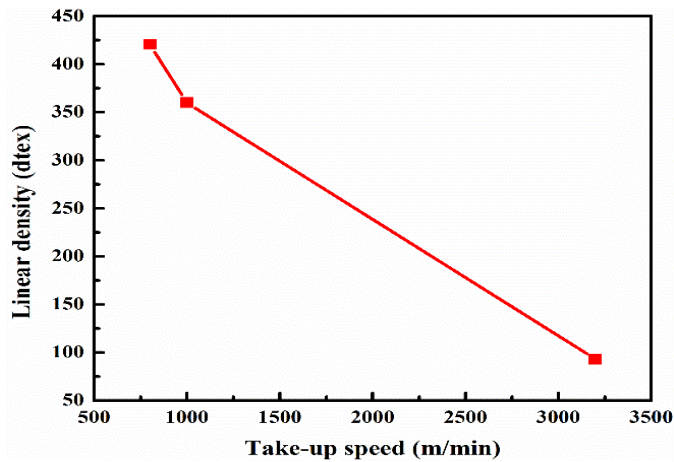


FIGURE 2. Fiber linear density at different take-up speeds

Morphological structure of PA56 as-spun fibers

Figure 3 shows the SEM images of the PA56 as-spun fibers prepared at different take up speeds at different magnifications. PA56 fibers have exhibited clean and smooth surface. It is clearly observed that the fiber diameter gradually decrease by increasing the take up speeds.

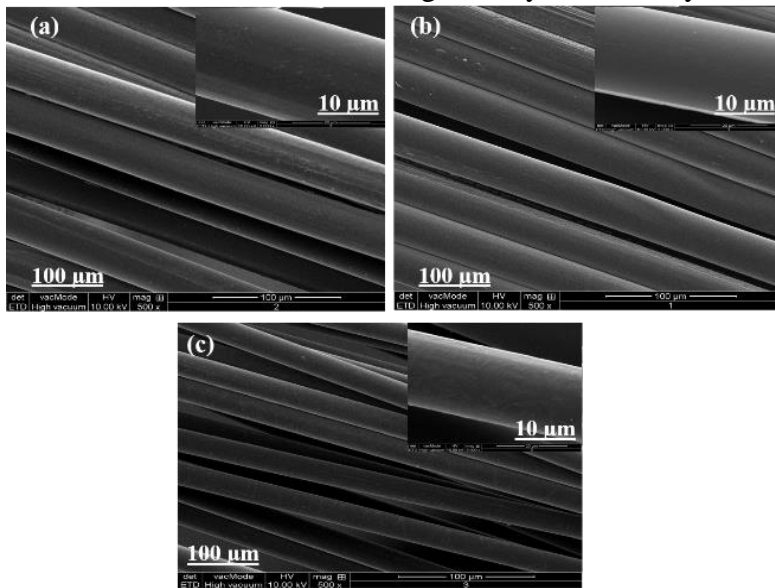


FIGURE 3. SEM images of PA56 as-spun fibers at different take up speeds (a) 800 m/min, (b) 1000 m/min and (c) 3200 m/min.

Thermal properties

It is well known that the thermal behavior of synthetic fibers changes according to the fiber processing conditions, such as take-up speed and spinning temperature. Figure 4 plots the differential scanning calorimetry (DSC) thermograms of PA56 as-spun fibers prepared with different take-up speeds. The DSC heating scan showed a single melting peak, which attributed to the melting of the crystalline structure developed during the DSC temperature scanning. The thermal properties of PA56 as-spun fibers were summarized in Table 1. The Tg was increased from 59.3 °C to 61.9 °C and 62.3 °C, respectively, with the take-up speeds increase from 800

m/min to 1000 m/min and 3200 m/min. This may be attributed to the degree of molecular orientation developed during the fibers spinning. Small peak at around 118 °C was also observed. They were decreased with the take up speeds, indicating that they are arising from melting of different imperfection crystal at different take-up speeds.

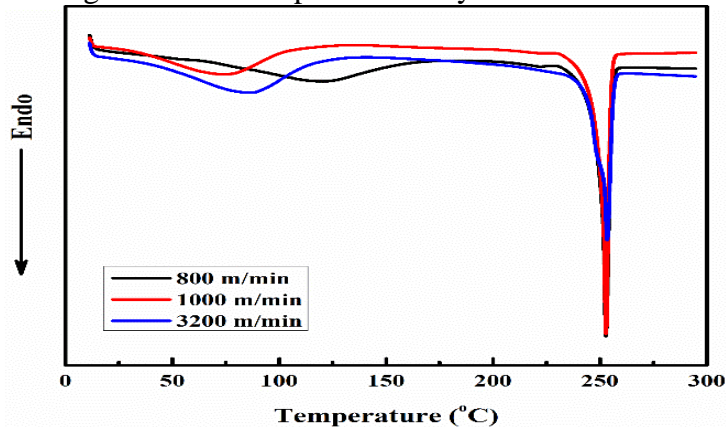


FIGURE 4. Thermograms of PA56 as-spun fibers at different take-up speeds

TABLE 1: DSC Thermodynamics parameters of PA56 as-spun fibers at different take-up speeds

Take-up Speed (m/min)	T _g (°C)	T _m (°C)	ΔH (J/g)
800	59.3	252.8	62.5
1000	61.9	252.9	66.2
3200	62.3	253.4	67.7

Dynamic mechanical thermal analysis (DMTA)

Dynamic mechanical analysis is one of the most powerful methods to investigate the variation of viscoelastic properties of polymeric materials with temperature. Figure 5 shows the storage modulus and tan δ of PA56 as-spun fibers with different take-up speeds. As shown in Figure 5(a), the storage modulus basically decreases with the temperature in the investigated temperature range. The characteristic evaluation of the storage modulus occurs in a temperature range of 60 to 120 °C. This transition is associated to the mobility of the amorphous region of the material. On the other hand, there is an increase in the total storage modulus with the increase of the take up speeds. Figure 5(b), shows the change in tan δ of PA56 fibers with different take-up speeds in the range of scanning temperature. The peak height of tan δ decreases with the take-up speeds. The values of the low temperature limit of storage limit and the peak values of the tan δ of PA56 as-spun fibers are summarized in Table 2.

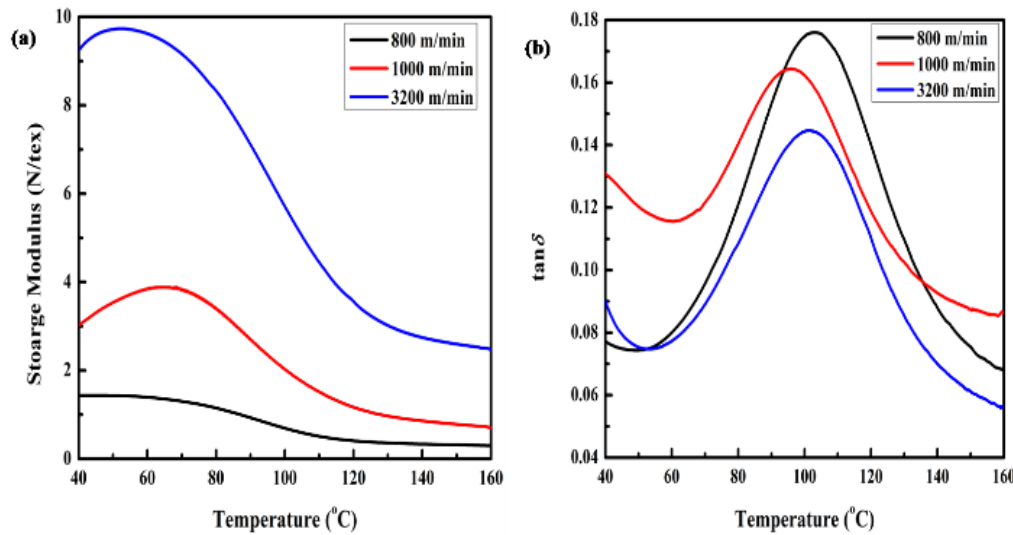


FIGURE 5. Dynamic mechanical behaviors of PA56 as-spun fibers at different take-up speed; (a) Storage modulus; (b) $\tan \delta$

TABLE 2. Glass transition temperature (T_g) values from storage modulus and $\tan \delta$ of PA56 as-spun fibers at different take-up speeds

<i>Take-up speed (m/min)</i>	<i>Storage modulus (N/tex)</i>	<i>$\tan \delta$</i>
PA56-800	69.9°C	102.9 °C
PA56-1000	74.5°C	96.2 °C
PA56-3200	72.5°C	101.5 °C

Crystal structure of PA 56 as-spun fibers

The one-dimensional equatorial (WAXD) scanning patterns of PA56 as-spun fibers prepared at different take-up speeds are shown in *Figure 6*. As shown in *Figure 6*, the WAXD data shows two main characteristic diffraction peaks located at 2θ values of around 20.3° and 22.6° , correspond to d-spacing of 0.43 and 0.39 nm, respectively, which were assigned to the (020) and (110) planes, respectively (Puiggali *et al.*, 1998). This result is out of expectation as odd-even nylons typically exhibit the γ -structure characterized by a single reflection with a d-spacing of 0.415 nm. Other investigators have observed crystal structures for odd-even polyamides that deviate from the γ -form. Two strong diffraction signals close to the characteristic spacings of the α -form has been observed for nylon 5,10 (Villaseñoret *et al.*, 1999), nylon 9,2 (Franco *et al.*, 1998), nylon 11,10 (Cui and Yan, 2005), nylon 11,12 (Cui and Yan, 2005), and nylon 13,6 (Samanta *et al.*, 2013). Thus, the WAXD data obtained for PA56 appears to be consistent with the results obtained for other odd-even polyamides that do not exhibit the pattern consistent with the γ -form.

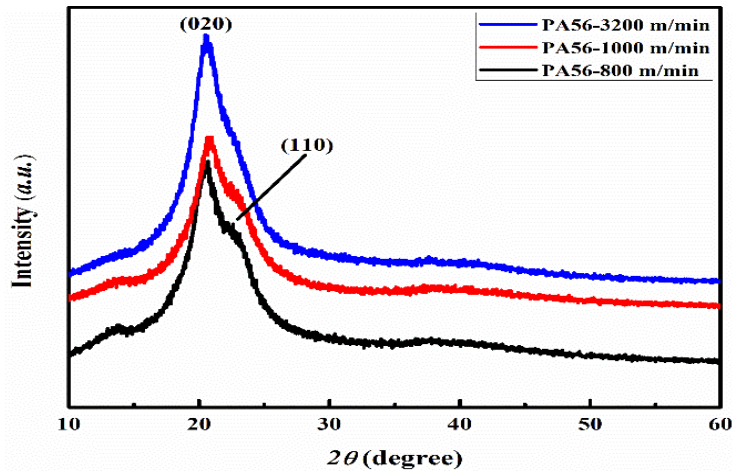


FIGURE 6. WAXD patterns for PA56 as-spun fibers at different take-up speeds

The crystallite size perpendicular to the (020) plane is obtained from the half width of the peak in the 2θ scanning by using the Scherrer equation (Patterson, 1939). The relative crystallinity and crystal size are shown in *Figure 7*. It could be seen that the relative crystallinity of PA56 as-spun fibers increased from 33.34% to 33.56% and 38.03%, respectively, with the take-up speeds. On the other hand, the crystal sizes increase from 3.49 nm to 3.52 nm and 4.23 nm, respectively, with the take-up speeds. At higher take-up speeds, higher spin-line stresses on the filaments leads to improvement in the molecular orientation along the fiber axis, which results in the increase of the crystallinity and crystal sizes. Shimizu et al. (Shimizu *et al.*, 1981) reported that the crystallinity of nylon 6 sharply increased at take-up speeds higher than 3000 m/min.



FIGURE 7. Relative crystallinity and crystal size versus take-up speeds

Molecular orientation (f_0)

The molecular orientation (f_0) values of PA56 as-spun fibers at different take-up speeds are measured by a sound velocity apparatus and plotted in *Figure 8*. The results reveal that the molecular orientation (f_0) of PA56 fibers increases quickly with the increase of take-up speeds from 800 to 1000 m/min, and then increased when the take-up speed increased to 3200 m/min. This may be attributed to an increase of molecular orientation in non-crystalline regions with the

take-up speeds due to the increase of the spinline tension and the difference between the take-up and extrusion velocities.

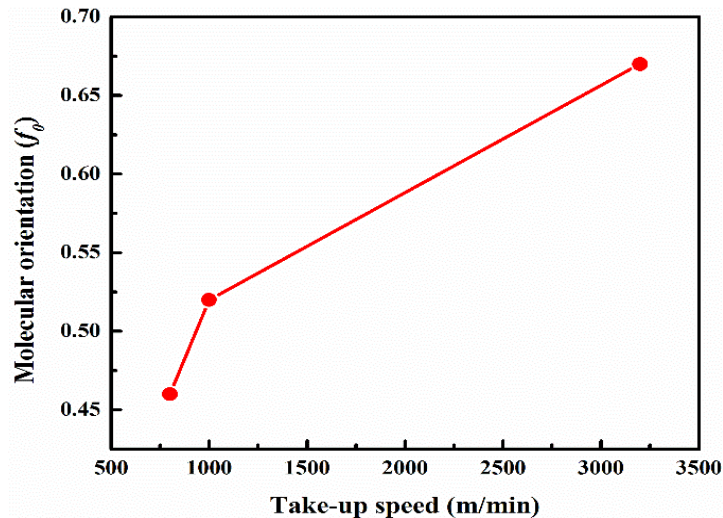


FIGURE 8. Plot of molecular orientation (f_0) at different take-up speeds
Study of dyeability of PA56

In order to study the dyeability of PA56 knitted fabrics, the dyeing process was carried out using an acid dyes, which are the most widely used dyes for polyamides. These dyes react with the end amine groups of polyamide forming ionic bonds between the dye molecules and polymer chains. *Figure 9* shows the effect of take-up speeds on dyebath exhaustion of PA56 knitted fabrics dyed with C.I. Acid Red 88 dye. It is apparent from *Figure 9* that the dyebath exhaustion decreased from 92.8% to 87.5% and 75.8%, respectively, as the take-up speeds increased from 800 m/min to 1000 m/min and 3200 m/min. As revealed by the wide-angle x-ray diffractions (WAXD) and sonic velocity measurements, the relative crystallinity and molecular orientation increases with increasing take-up speeds. Therefore, the decrease of dye exhaustion should be attributed to the increase in crystallinity and molecular orientation with take up speeds. Vasanthan and Huang (Vasanthan and Huang, 2003) reported that the dye diffusion coefficient of PA66 decreased with increasing the volume fraction crystallinity and amorphous orientation originated from heat setting and drawing process.

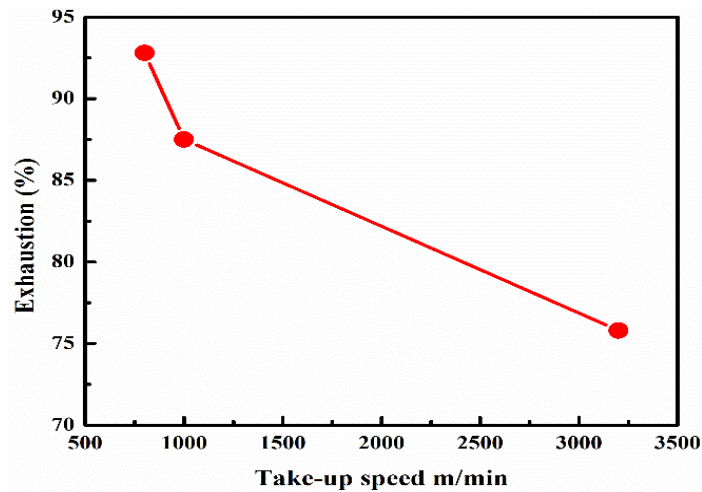


FIGURE 9. Effect of take-up speeds on dyebath exhaustion

The color strength (K/S) results for PA56 knitted fabrics prepared at different take-up speeds are shown in *Figure 10*. It could be seen that the color strength (K/S) value decreased from 35.4 to 35.1 and 32.96, respectively, as the take-up speeds increased from 800 m/min to 1000 m/min and 3200 m/min. The decrease in color strength could be attributed to the structural and morphological changes in terms of changes in crystallinity, crystal sizes and molecular orientation with the take-up speeds.

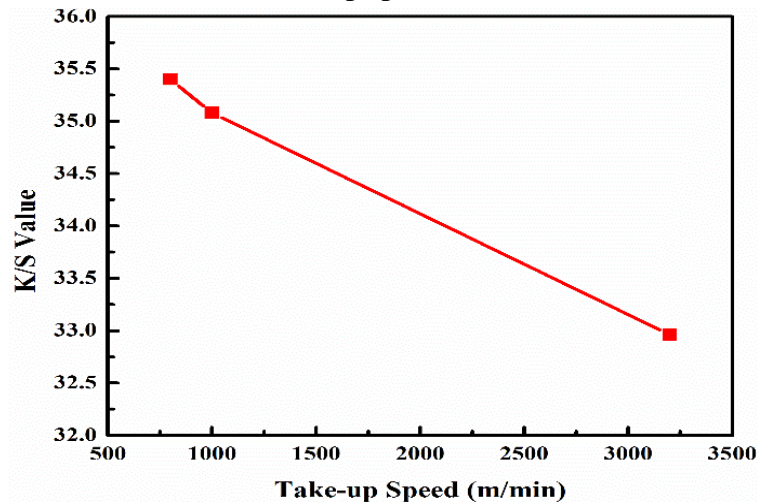


FIGURE 10. Effect of take-up speeds on color strength (K/S)

CONCLUSIONS

Polyamide 5,6 (PA56) as-spun fibers were prepared successfully by melt spinning process at different take-up speeds. The effects of take-up speeds on structure of PA56 spun fibers were investigated by means of DSC, DMTA, wide-angle x-ray diffractions (WAXD) and sonic velocity measurements. In addition, the PA56 knitted fabrics were dyed with C.I. Acid Red 88 dye and the dyeability were evaluated by color strength (K/S) measurements. The results reveal that the glass transition temperature (T_g) increases, while the melting temperature shows no considerable variation with the take-up speeds. The storage modulus decreases along the temperature range investigated and the peak height of $\tan \delta$ decreases with take-up speeds. The

equatorial (WAXD) data of PA56 exhibit characteristic peaks at 2θ values of approximately 20.3° and 22.6° , which correspond to d-spacing of 0.43 and 0.39 nm, respectively. This is similar to a characteristic of the α -like crystal structure of many odd-even nylons such as nylon 5,10, nylon 9,2 and nylon 11,10. It is also found that the relative crystallinity, crystal sizes and molecular orientation of PA56 as-spun fibers increase with take-up speeds due to the increased stress-induced crystallization along with the increasing spinline stress with take-up speeds. The dyebath exhaustion and color strength (K/S) values decreased with take-up speeds. This could be arising from the increase in crystallinity and molecular orientation.

REFERENCES

- Alexander, Leroy Elbert. (1969). *X-ray diffraction methods in polymer science*: Wiley-Interscience New York.
- Anton, Anthony, & Baird, Bennett R. (2002). Polyamides, Fibers *Encyclopedia of Polymer Science and Technology*: John Wiley & Sons, Inc.
- Arimoto, H. (1964). α - γ Transition of nylon 6. *Journal of Polymer Science Part A: General Papers*, 2(5), 2283-2295.
- Atav, Rıza, Çay, Ahmet, Körlü, Ayşegül Ekmekçi, & Duran, Kerim. (2006). Comparison of the effects of various presettings on the colour of polyamide 6.6 dyed with acid dyestuffs. *Coloration Technology*, 122(5), 277-281.
- Bankar, Vilas G., Spruiell, Joseph E., & White, James L. (1977). Melt spinning of nylon 6: Structure development and mechanical properties of as-spun filaments. *Journal of Applied Polymer Science*, 21(9), 2341-2358.
- Bolton, E. K. (1942). Chemical Industry Medal. Development of Nylon. *Industrial & Engineering Chemistry*, 34(1), 53-58.
- Bunn, C. W., & Garner, E. V. (1947). The Crystal Structures of Two Polyamides ('Nylons'). *Proceedings of the Royal Society of London. Series A. Mathematical and Physical Sciences*, 189(1016), 39-68.
- Carothers W.H., U.S. Patent 1938; 2,130,948.
- Carothers W.H., Graves GD., U.S. Patent, 1939; 2 163 584.
- Carothers, Wallace H., & Hill, Julian W. (1932). STUDIES OF POLYMERIZATION AND RING FORMATION. XV. ARTIFICIAL FIBERS FROM SYNTHETIC LINEAR CONDENSATION SUPERPOLYMERS. *Journal of the American Chemical Society*, 54(4), 1579-1587.
- Carothers, Wallace H., & Natta, Frank J. van. (1933). Studies of Polymerization and Ring Formation. XVIII. Polyesters from ϵ -Hydroxydecanoic Acid. *Journal of the American Chemical Society*, 55(11), 4714-4719.
- Cui, X., & Yan, D. (2005). Preparation, characterization and crystalline transitions of odd-even polyamides 11,12 and 11,10. *European Polymer Journal*, 41(4), 863-870.
- Danford, Merlin D., Spruiell, Joseph E., & White, James L. (1978). Structure development in the melt spinning of nylon 66 fibers and comparison to nylon 6. *Journal of Applied Polymer Science*, 22(12), 3351-3361.
- Eltahir, Yassir A., Saeed, Haroon A. M., Xia, Yumin, Yong, He, & Yimin, Wang. (2016). Mechanical properties, moisture absorption, and dyeability of polyamide 5,6 fibers. *The Journal of The Textile Institute*, 107(2), 208-214. doi: 10.1080/00405000.2015.1020678

- Franco, L., Subirana, J. A., & Puiggali, J. (1998). Structure and morphology of odd polyoxamides [Nylon 9,2]. A new example of hydrogen-bonding interactions in two different directions. *Macromolecules*, 31(12), 3912-3924.
- Kind, Stefanie, Neubauer, Steffi, Becker, Judith, Yamamoto, Motonori, Völkert, Martin, Abendroth, Gregory von, Wittmann, Christoph. (2014). From zero to hero – Production of bio-based nylon from renewable resources using engineered *Corynebacterium glutamicum*. *Metabolic Engineering*, 25(0), 113-123. doi:http://dx.doi.org/10.1016/j.ymben.2014.05.007
- Kind, Stefanie, & Wittmann, Christoph. (2011). Bio-based production of the platform chemical 1,5-diaminopentane. *Applied Microbiology and Biotechnology*, 91(5), 1287-1296.
- Kinoshita, Yukio. (1959a). The crystal structure of polyheptamethylene pimelamide (nylon 77). *Die Makromolekulare Chemie*, 33(1), 21-31.
- Kinoshita, Yukio. (1959b). An investigation of the structures of polyamide series. *Die Makromolekulare Chemie*, 33(1), 1-20.
- Kohan, Melvin I. (1995). *Nylon plastics handbook* (Vol. 378): Hanser Publishers Munich, Germany, Vienna, and New York.
- Lu, Shengjun, Zhou, Zhimin, Yu, Jie, Li, Fei, & He, Min. (2013). Study on the Influence of Crystal Structures on the Performance of Low-Melting Polyamide 6. *Polymer-Plastics Technology and Engineering*, 52(2), 157-162.
- Morales-Gámez, Laura, Soto, David, Franco, Lourdes, & Puiggali, Jordi. (2010). Brill transition and melt crystallization of nylon 56: An odd–even polyamide with two hydrogen-bonding directions. *Polymer*, 51(24), 5788-5798.
- Patterson, AL. (1939). The Scherrer formula for X-ray particle size determination. *Physical review*, 56(10), 978.
- Puiggali, J., Franco, L., Alemán, C., & Subirana, J. A. (1998). Crystal Structures of Nylon 5,6. A Model with Two Hydrogen Bond Directions for Nylons Derived from Odd Diamines. *Macromolecules*, 31(24), 8540-8548.
- Rahbar, Ruhollah Semnani, & Haji, Aminoddin. (2013). Use of D-optimal design to model and the analysis of the effect of the draw ratio on some physical properties of hot multistage drawn nylon 6 fibers. *Journal of Applied Polymer Science*, 130(2), 1337-1344.
- Samanta, Satyabrata, He, Jie, Selvakumar, Sermadurai, Lattimer, Jessica, Ulven, Chad, Sibi, Mukund, Chisholm, Bret J. (2013). Polyamides based on the renewable monomer, 1,13-tridecane diamine II: Synthesis and characterization of nylon 13,6. *Polymer*, 54(3), 1141-1149.
- Samon, Joshua M., Schultz, Jerold M., Wu, Jing, Hsiao, Benjamin, Yeh, Fengji, & Kolb, Rainer. (1999). Study of the structure development during the melt spinning of nylon 6 fiber by on-line wide-angle synchrotron X-ray scattering techniques. *Journal of Polymer Science Part B: Polymer Physics*, 37(12), 1277-1287.

- Shimizu, Jiro, Okui, Norimasa, Kikutani, Takeshi, Ono, Akihiro, & Takaku, Akira. (1981). High speed melt spinning of nylon 6. *Sen'i Gakkaishi*, 37(Copyright (C) 2013 American Chemical Society (ACS). T143-T152.
- Stepaniak, R. F., Garton, A., Carlsson, D. J., & Wiles, D. M. (1979). The characterization of nylon 6 filaments by x-ray diffraction. *Journal of Applied Polymer Science*, 23(6), 1747-1757.
- Vasanthan, Nadarajah, & Huang, Xin-Xian. (2003). Effect of polymer microstructure on dye diffusion in polyamide 66 fibers. *Journal of Applied Polymer Science*, 89(14), 3803-3807.
- Villaseñor, P., Franco, L., Subirana, J. A., & Puiggalí, J. (1999). On the crystal structure of odd-even nylons: Polymorphism of nylon 5,10. *Journal of Polymer Science, Part B: Polymer Physics*, 37(17), 2383-2395.
- Ziabicki, Andrzej, & Kedzierska, Krystyna. (1959). Studies on the orientation phenomena by fiber formation from polymer melts. Part I. Preliminary investigations on polycapronamide. *Journal of Applied Polymer Science*, 2(4), 14-23.

تأثير سرعة إنتاج الشعيرات على البنية التركيبية والخواص والقابلية للصبغة لشعيرات البولي أميد 6,5 (النايلون 6,5)

الخلاصة

تم تحضير شعيرات البولي أميد 6,5 (النايلون 6,5) بنجاح باستخدام عملية الغزل الإنصهاري وتم دراسة أثر سرعة إنتاج الشعيرات على الخواص الحرارية، والبنية البلورية، والقابلية للصبغة بواسطة جهاز المسح المسعري التفاضلي (DSC)، وحيود الأشعة السينية (WAXD)، والتحليل الحراري الميكانيكي الديناميكي (DMTA)، والسرعة الصوتية (Sonic velocity) وقوة اللون (ColorStrength). أظهرت نتائج جهاز المسح المسعري التفاضلي (DSC) أن درجة حرارة الانتقال الزجاجية (Tg) لشعيرات البولي أميد 6,5 ازدادت، بينما لا تُظهر درجة حرارة الانصهار أي اختلاف كبير مع زيادة سرعة الإنتاج. تبين نتائج التحليل الحراري الميكانيكي الديناميكي (DMTA) ازدياد معامل التخزين، وانخفاض قمة إرتفاع $\tan\delta$ مع سرعات الإنتاج. يُظهر حيود الأشعة السينية (WAXD) للبولي أميد 6,5 بنية تركيبية شبه الفا (α -like)، كما هو ملاحظ في النايلونات الفردية-الزوجية مثل النايلون 10,5، والنايلون 2,9 وهكذا. وقد وجد أيضاً التبلور النسبي، واحجام البلورات وتوجه الجزيئات لشعيرات البولي أميد 6,5 قد ازدادت مع زيادة سرعة الإنتاج. ونتيجة لذلك، انخفضت قيم الإستنفاد لحمام الصبغة وقوة اللون (K/S).